# Simulation of the crystallization process of $Ge_2Sb_2Te_5$ nanoconfined in superlattice geometries for phase change memories Supplementary Information

Debdipto Acharya, Omar Abou El Kheir, Simone Marcorini, and Marco Bernasconi*

*Department of Materials Science, University of Milano-Bicocca, Via R. Cozzi 55, I-20125 Milano, Italy*

E-mail: marco.bernasconi@unimib.it

Table S1: Average coordination number for different pairs of atoms computed from the partial pair correlation functions for models of amorphous GST generated with and without (from Ref.[1]) vdW corrections, both at the experimental density of the amorphous phase of 0.0309 atom/Å$^3$ (bulk-LD). The theoretical results are compared with experimental data from anomalous x-ray scattering (AXS),[2] extended x-ray absorption spectroscopy (EXAFS),[3] and reverse Monte-Carlo (RMC) analysis of combined x-ray and neutron diffraction and EXAFS.[4] A more comprehensive comparison of experimental data with previous DFT calculations with PBE and other functionals is reported in a very recent work (see Table 5 in Ref.[5]). To determine the coordination numbers, we used 3.2 Å as a bond cutoff for all pairs except for Te-Sb for which we used 3.4 Å. In the experimental work of Ref.[4] they used as cutoff the first minimum of the pair correlation functions corresponding to (Ge-Ge) 3.05 Å, (Sb-Ge) 3.18 Å, (Te-Ge) 3.18 Å, (Sb-Sb) 3.28 Å, (Te-Te) 3.29 Å, and (Te-Sb) 3.35 Å. For the sake of comparison, we report in the last column the coordination numbers of our models computed with the cutoffs of Ref.[4] .

| | | NN | NN+vdW | AXS[2] | EXAFS[3] | RMC[4] | NN+vdW (cutoff of Ref.[4]) |
|---|---|---|---|---|---|---|---|
| Ge | with Ge | 0.33 | 0.33 | 0.7 | 0.6 | 0.69 | 0.31 |
| | with Sb | 0.30 | 0.33 | | 0.0 | 0.83 | 0.30 |
| | with Te | 3.35 | 3.53 | 3.26 | 3.3 | 2.72 | 3.31 |
| | Total | 3.99 | 4.19 | 4.24 | 3.9 | 4.24 | 3.92 |
| Sb | with Ge | 0.30 | 0.33 | | 0.0 | 0.83 | 0.30 |
| | with Sb | 0.55 | 0.51 | | 0.0 | 0.00 | 0.58 |
| | with Te | 3.20 | 3.64 | 2.51 | 2.8 | 2.39 | 3.08 |
| | Total | 4.06 | 4.46 | 2.95 | 2.8 | 3.22 | 3.96 |
| Te | with Ge | 1.34 | 1.41 | 1.30 | 1.2 | 1.08 | 1.33 |
| | with Sb | 1.28 | 1.45 | 1.00 | 1.2 | 0.96 | 1.23 |
| | with Te | 0.31 | 0.29 | | 0.0 | 0.00 | 0.37 |
| | Total | 2.93 | 3.16 | 2.30 | 2.4 | 2.04 | 2.93 |

Table S2: Position (Å) of the first maximum of the partial pair correlation functions for models of amorphous GST generated with and without (from Ref.[1]) vdW corrections, both at the experimental density of the amorphous phase of 0.0309 atom/Å$^3$ (bulk-LD). The theoretical results are compared with experimental data from anomalous x-ray scattering (AXS),[2] extended x-ray absorption spectroscopy (EXAFS),[3] and reverse Monte-Carlo (RMC) analysis of combined x-ray and neutron diffraction and EXAFS.[4] A more comprehensive comparison of experimental data with previous DFT calculations with PBE and other functionals is reported in a very recent work (see Table 5 in Ref.[5]).

| | | NN | NN+vdW | AXS[2] | EXAFS[3] | RMC[4] |
|---|---|---|---|---|---|---|
| Ge | with Ge | 2.62 | 2.61 | 2.50 | 2.47 | 2.48 |
| | with Sb | 2.82 | 2.80 | | 2.69 | |
| | with Te | 2.78 | 2.76 | 2.65 | 2.63 | 2.64 |
| Sb | with Sb | 2.99 | 2.99 | | | |
| | with Te | 2.96 | 2.92 | 2.82 | 2.83 | 2.83 |
| Te | with Te | 3.04 | 2.95 | | | |

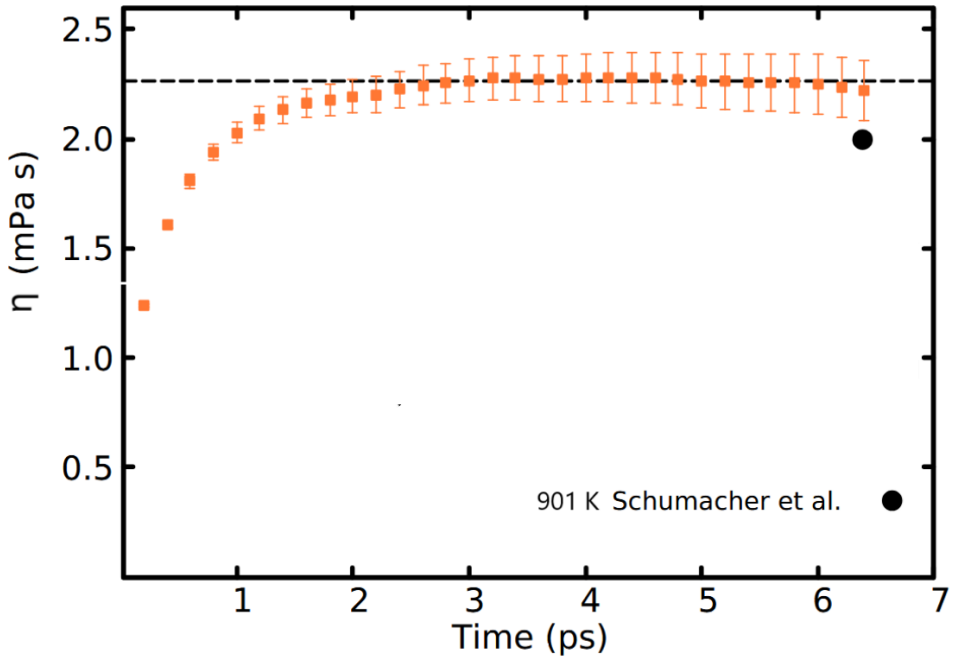


Figure S1: Viscosity $\eta$ of GST at 900 K at the experimental density of the liquid. The value of $\eta(t)$ is shown as a function of the integration time $t$ in the Green-Kubo formula $\eta = \lim_{t\to\infty} \frac{V}{k_B T} \int_0^t \langle \sigma_{xy}(t' + t_o)\sigma_{xy}(t_o)\rangle dt' = \lim_{t\to\infty} \eta(t)$, where $V$ is the supercell volume, $T$ is the temperature, and $\sigma_{xy}$ is the off-diagonal component of the stress tensor. The average $\langle \dots \rangle$ is over the initial times $t_o$. We also took an average over the three off-diagonal components $xy$, $xz$, and $yz$. In practice, $\eta$ is evaluated from the plateau in the value of $\eta(t)$ at intermediate times, while at longer times the integral does not necessarily converge due to accumulation of noise.[6] We choose a maximum $t_{max}$ to evaluate $\eta(t)$ equal to twice the time at which the correlation function $\langle \sigma_{xy}(t+t_o)\sigma_{xy}(t_o)\rangle$ goes to zero. We performed blocks averages by first averaging over $t_o$ in $\langle \sigma_{xy}(t+t_o)\sigma_{xy}(t_o)\rangle$ in blocks with time length of $2t_{max}$. We then obtain the average $\eta(t)$ resulting from the Green-Kubo formula and its mean square errors by averaging over blocks. The resulting estimate of $\eta$ from the plateau (dashed line) is $\eta$=2.3 $\pm$ 0.2 mPa·s to be compared with the experimental value of 2.0 mPa·s of Ref.[7]

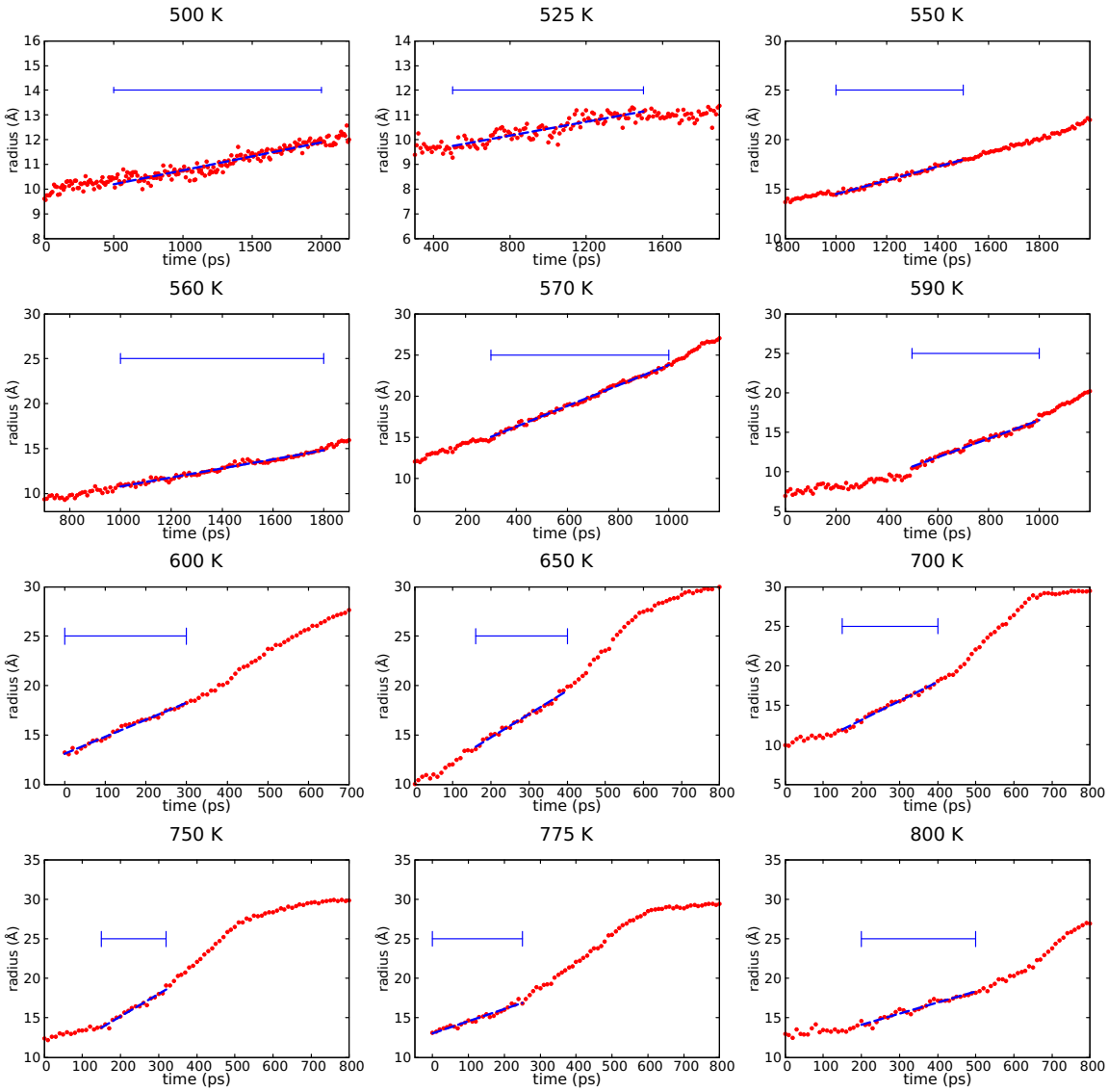


Figure S2: The evolution of the radius of the crystalline nuclei as a function of time in the NN+vdW simulations of the bulk at different temperatures and at the experimental density (bulk-LD). The linear fit in the range highlighted by horizontal bars yields the crystal growth velocity (see Table 3 in the article).

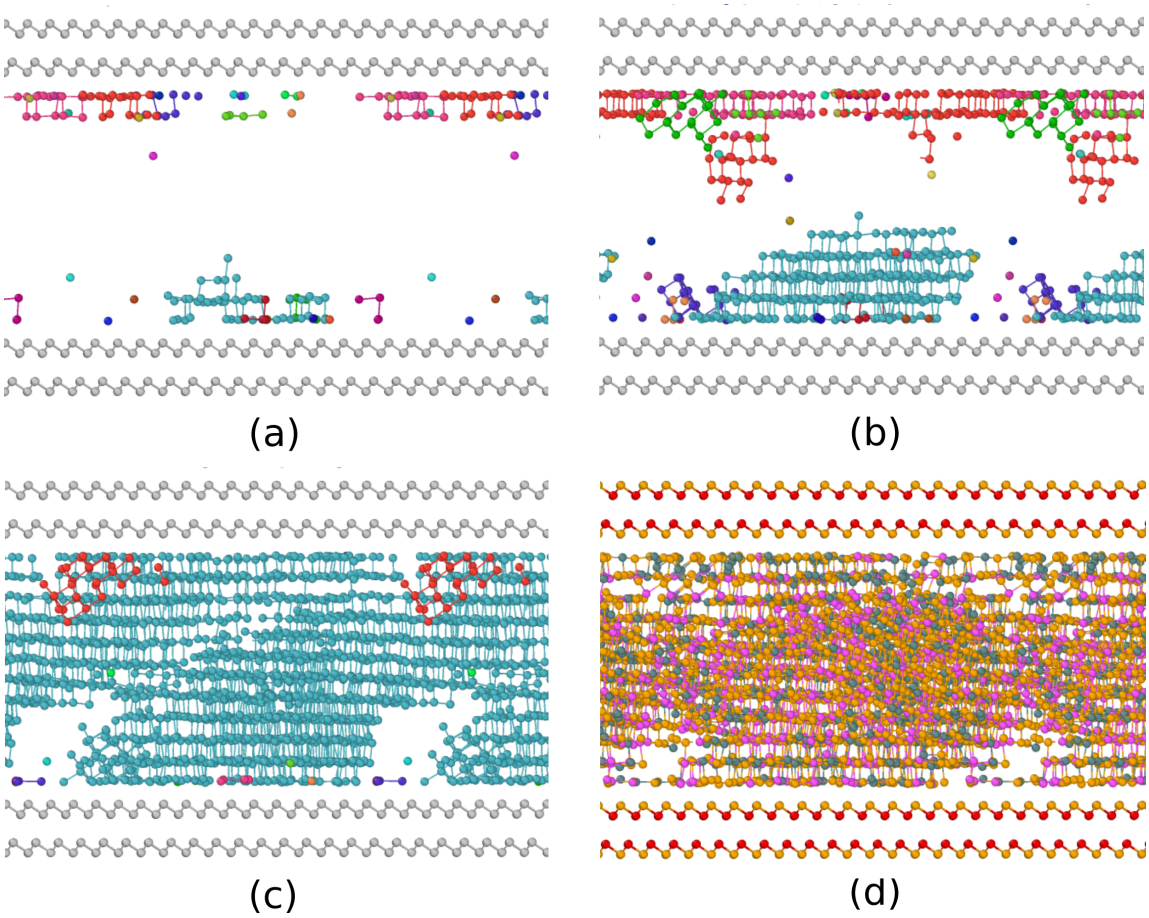


Figure S3: Simulation of the crystallization of a 3528-atom slab of amorphous GST capped by bilayers mimicking confinement by $TiTe_2$ in GST/$TiTe_2$-like SL (SL-HD). Snapshots at different times at 650 K are shown for (a) 0.5 ns, (b) 1 ns, and (c) 1.5 ns. Only crystalline atoms, identified by the $Q_4^{dot}$ order parameter (see article), are shown. Different crystalline nuclei have different colors. (d) Final configuration after 2 ns. The color code is the same of Fig. 1 of the article.

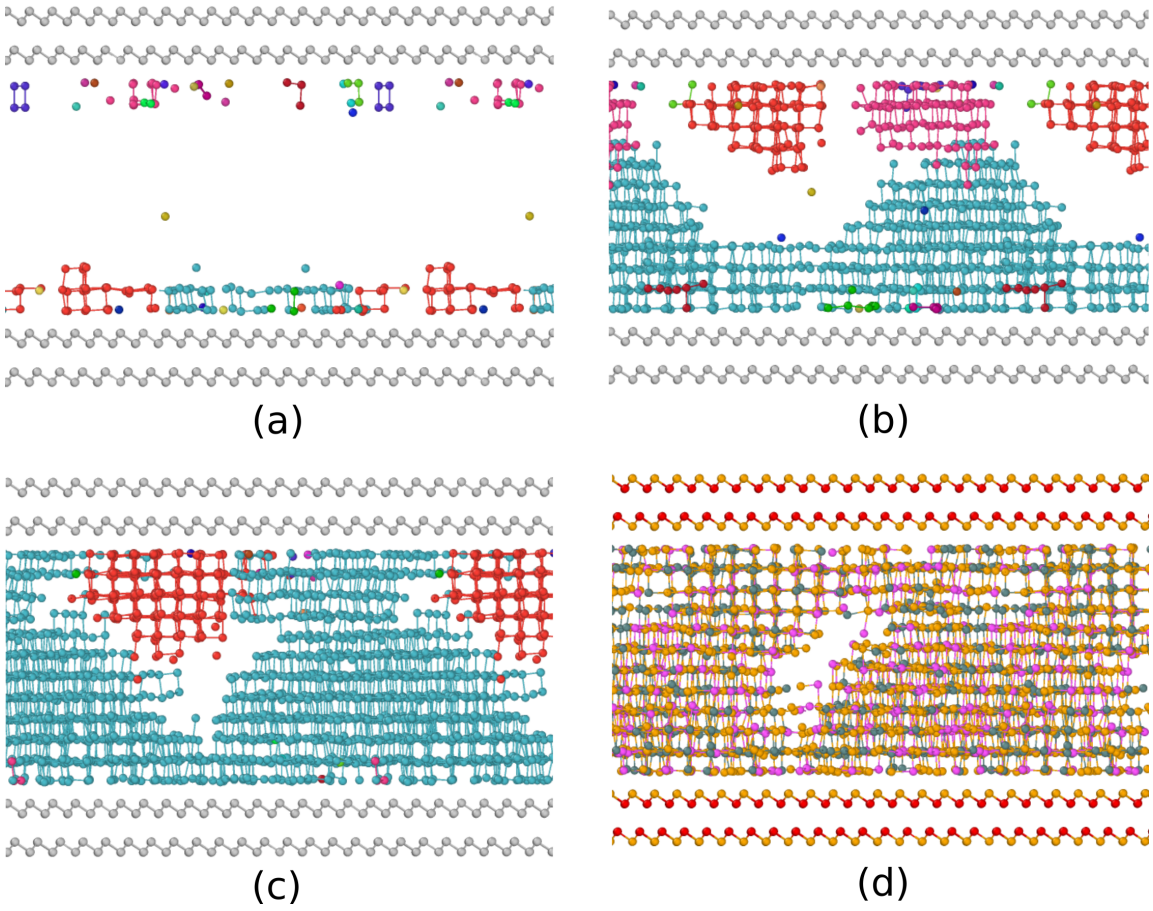


Figure S4: Simulation of the crystallization of a 3528-atom slab of amorphous GST capped by bilayers mimicking confinement by $TiTe_2$ in GST/$TiTe_2$-like SL (SL-HD). Snapshots at different times at 700 K are shown for (a) 0.5 ns, (b) 1 ns, and (c) 1.5 ns. Only crystalline atoms, identified by the $Q_4^{dot}$ order parameter (see article), are shown. Different crystalline nuclei have different colors. (d) Final configuration after 2 ns. The color code is the same of Fig. 1 of the article.

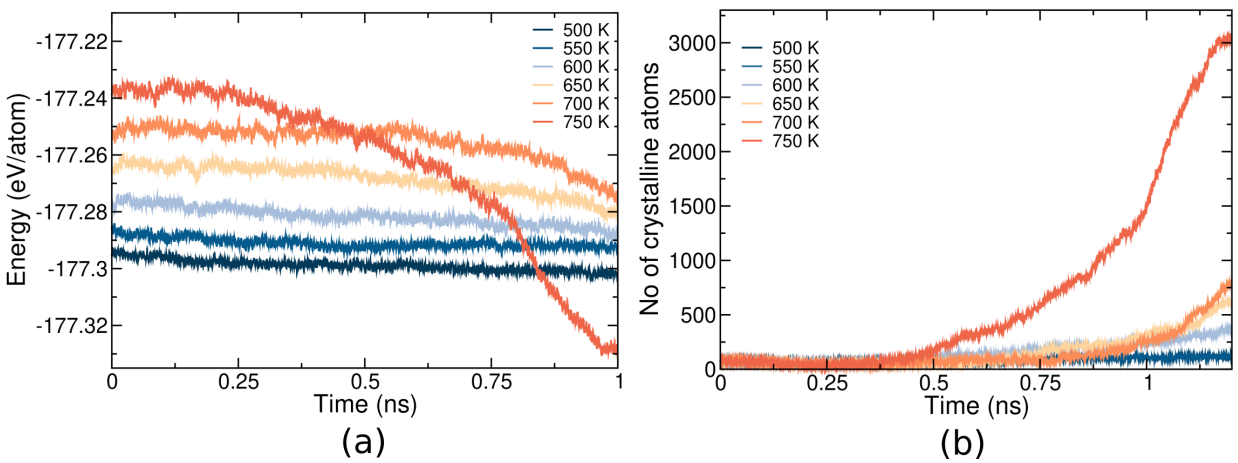


Figure S5: Crystallization of amorphous GST capped by bilayers mimicking confinement by $TiTe_2$ in GST/$TiTe_2$ SL at lower density (SL-LD', see text) at different temperatures. (a) Potential energy and (b) number of crystalline atoms as a function of time.

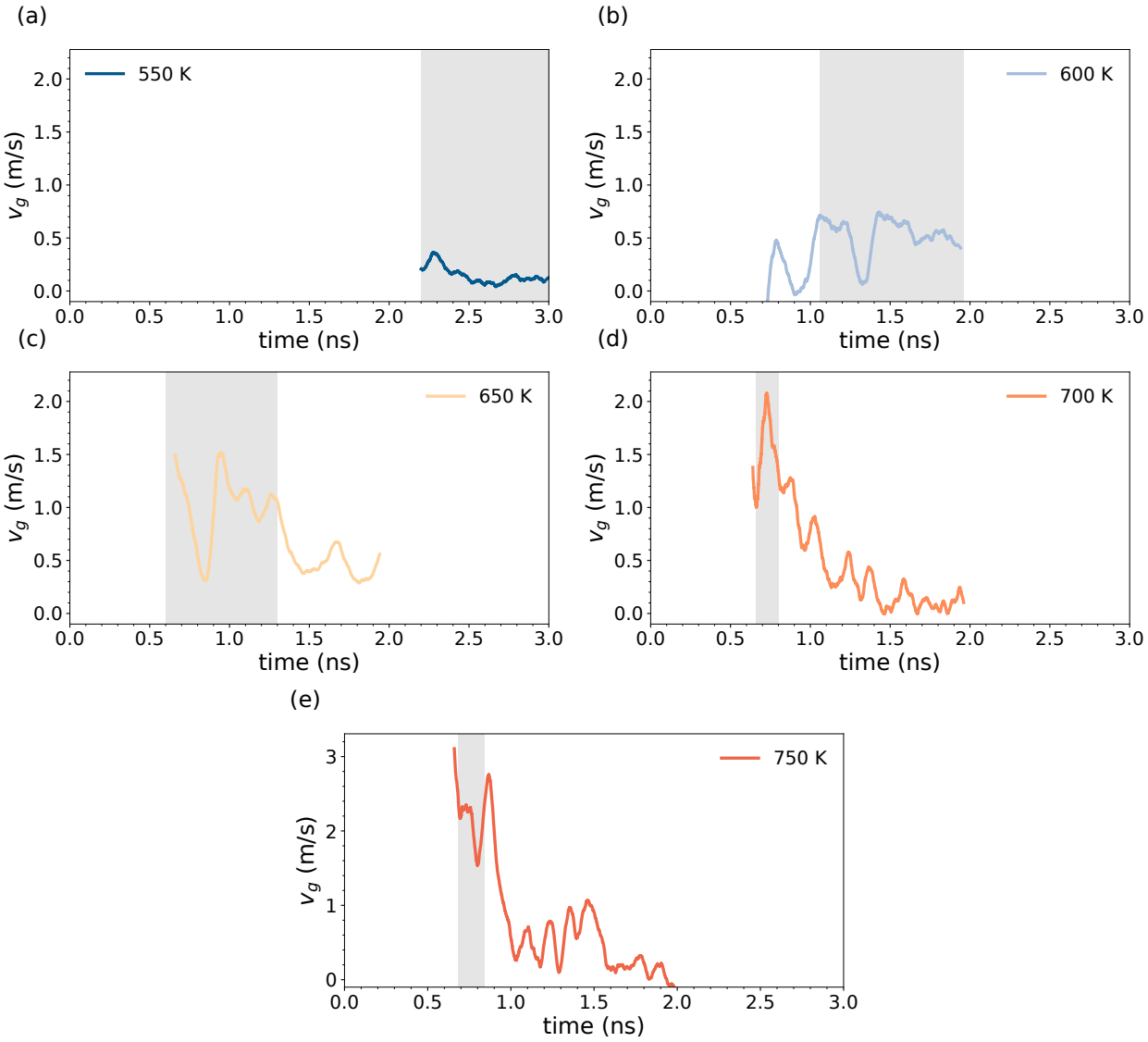


Figure S6: (a)-(e) Instantaneous crystal growth velocity ($v_g$) as a function of time at different temperatures for the SL-HD model. The region highlighted in gray corresponds to the time interval over which we estimated the average crystal growth velocities reported in Table 3 in the article.

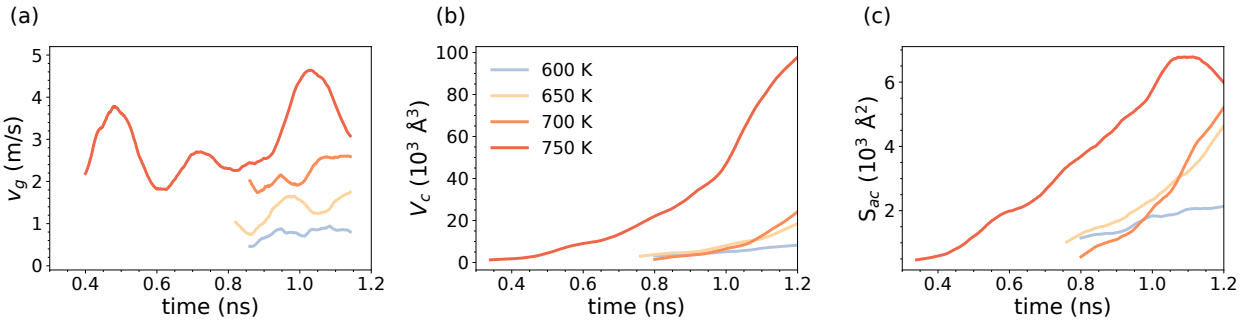


Figure S7: (a) Instantaneous crystal growth velocity $v_g$, (b) volume occupied by the crystalline atoms $V_c$ and (c) area of the crystal-amorphous interface $S_{ac}$ as a function of time at the different temperatures for the SL-LD' model.

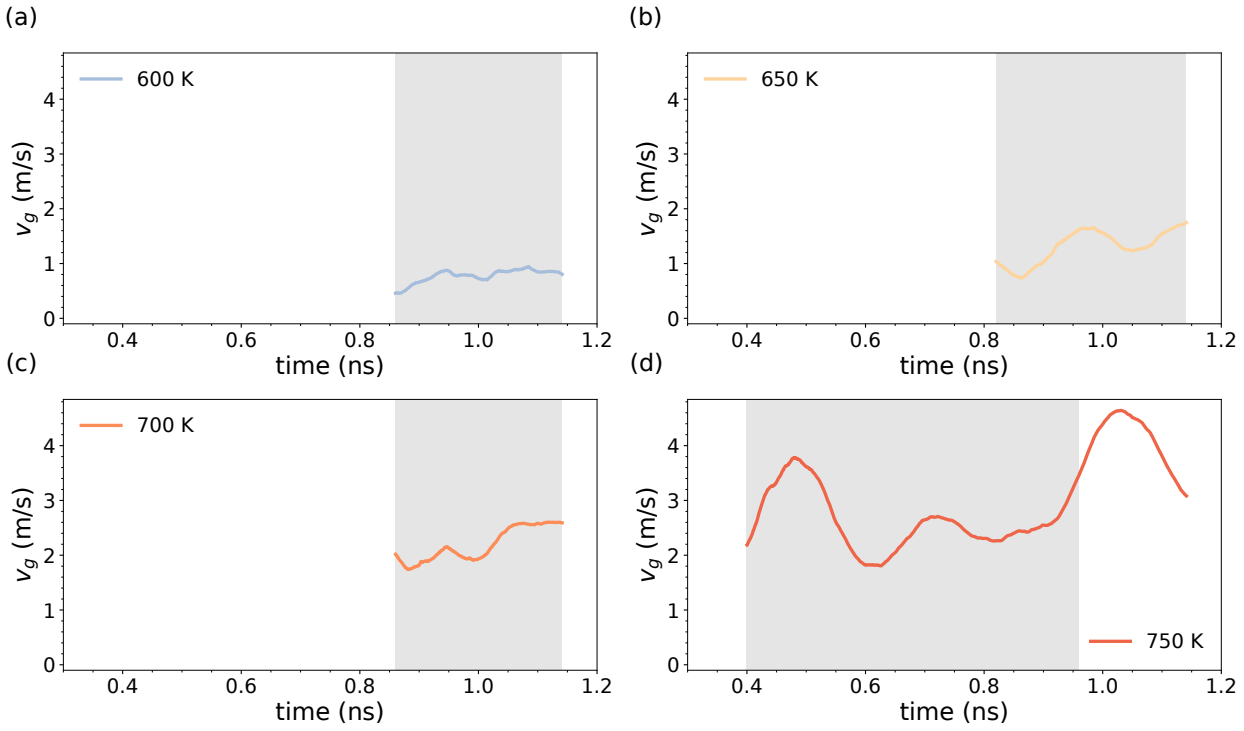


Figure S8: (a)-(d) Instantaneous crystal growth velocity ($v_g$) as a function of time at different temperatures for the SL-LD' model. The region highlighted in gray corresponds to the time interval over which we estimated the average crystal growth velocities reported in Table 3 in the article.

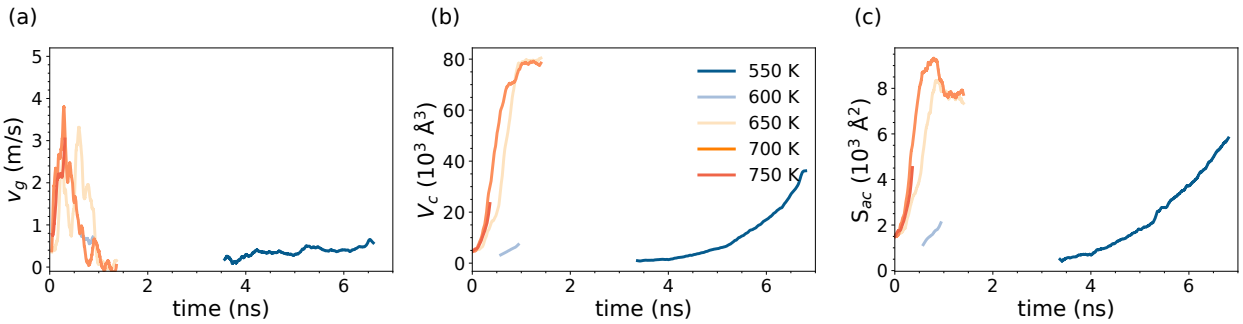


Figure S9: (a) Instantaneous crystal growth velocity $v_g$, (b) volume occupied by the crystalline atoms $V_c$ and (c) area of the crystal-amorphous interface $S_{ac}$ as a function of time at the different temperatures for the bulk simulations at low density (bulk-LD).

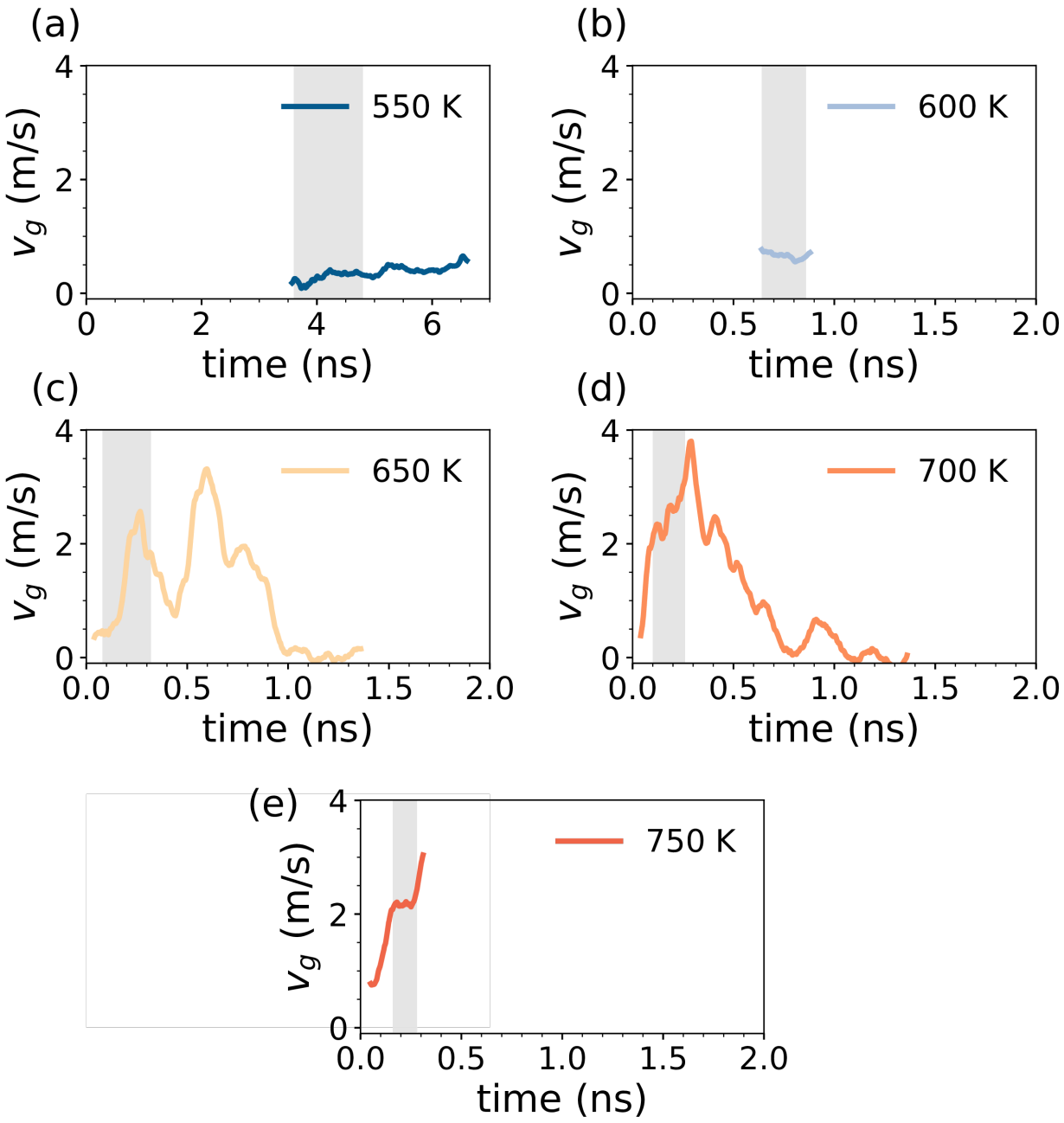


Figure S 10: (a)-(e) Instantaneous crystal growth velocity ($v_g$) as a function of time at different temperatures for the bulk at low density (bulk-LD). The region highlighted in gray corresponds to the time interval over which we estimated the average crystal growth velocities reported in Table 3 in the article.

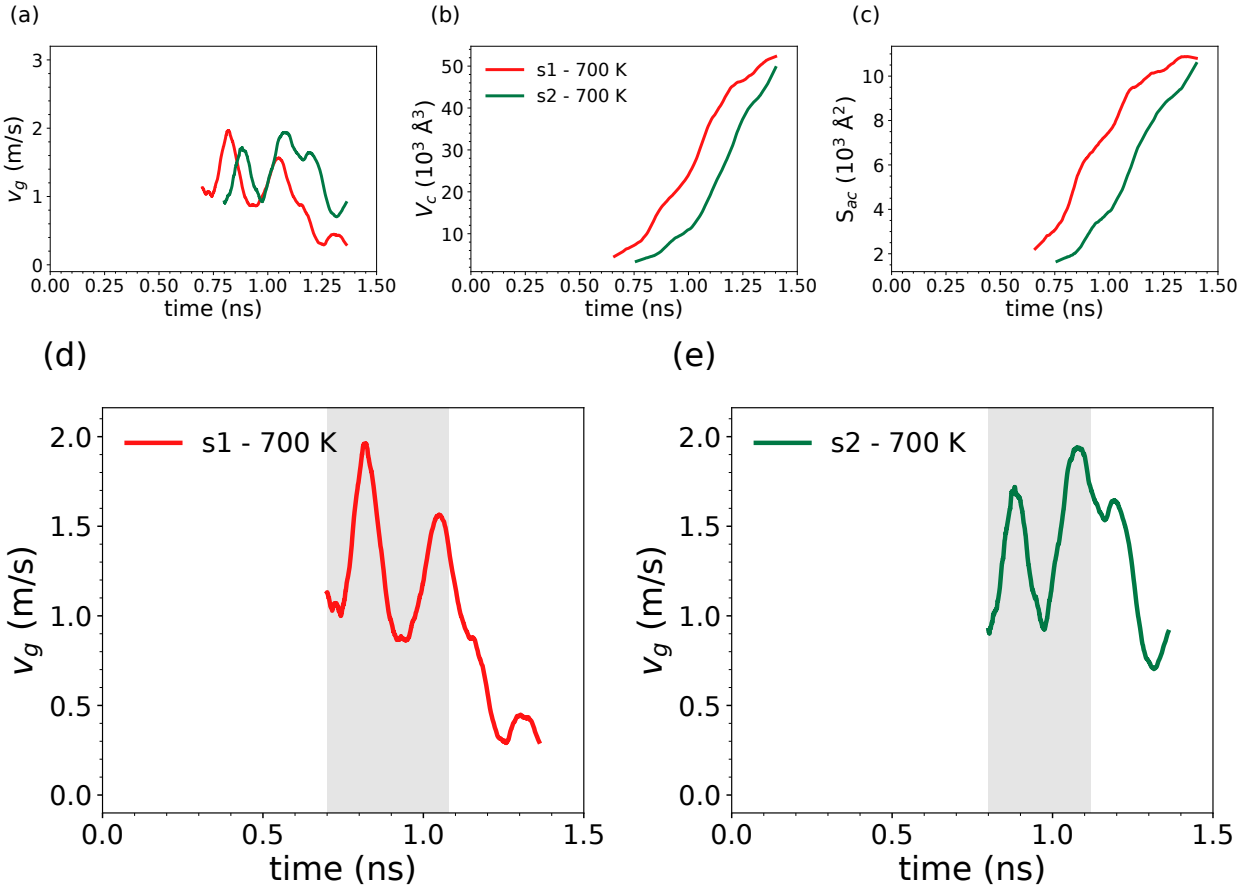


Figure S11: (a) Instantaneous crystal growth velocity $v_g$, (b) volume occupied by the crystalline atoms $V_c$, (c) area of the crystal-amorphous interface $S_{ac}$ as a function of time at 700 K in other two independent models for the SL-HD geometry. (d)-(e) Instantaneous crystal growth velocity ($v_g$) as a function of time where region highlighted in gray corresponds to the time interval over which we estimated the average crystal growth velocities reported in Table 3 in the article.

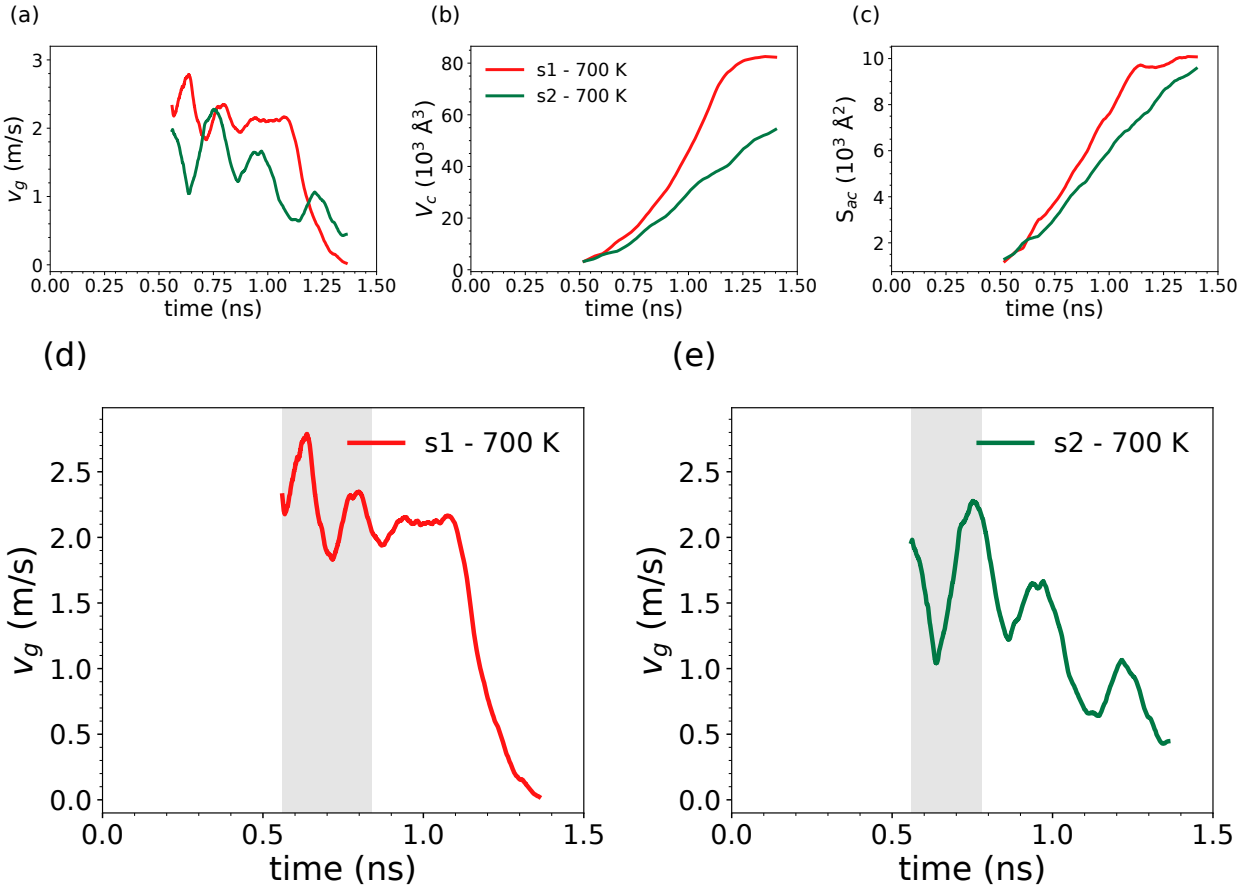


Figure S12: (a) Instantaneous crystal growth velocity $v_g$, (b) volume occupied by the crystalline atoms $V_c$, (c) area of the crystal-amorphous interface $S_{ac}$ as a function of time at 700 K in other two independent models of the SL-LD' geometry. (d)-(e) Instantaneous crystal growth velocity ($v_g$) as a function of time where region highlighted in gray corresponds to the time interval over which we estimated the average crystal growth velocities reported in Table 3 in the article.

Table S3: Two-dimensional diffusion coefficient $D$ as a function of time of the SL at the equilibrium density of the hexagonal phase (SL-HD, see article), from NVE simulations at the average temperatures given in the first column. We computed $D$ from the two dimensional mean square displacement (MSD) in the plane perpendicular to the slab thickness in the SL as $< x^2 > + < y^2 >= 4Dt$. The diffusion coefficient in the slab is compared to those in the bulk at the same density (bulk-HD, see article) at the average temperatures given in the third column. The calculations refer to amorphous models equilibrated at 300 K and then heated and equilibrated at the target temperature in 100 ps. D was then computed in the subsequent NVE simulations lasting 400 ps.

| Temperature (K) | $D$ ($10^{-6}$cm$^2$/s) SL-HD | Temperature (K) | $D$ ($10^{-6}$cm$^2$/s) Bulk-HD |
|---|---|---|---|
| 517 | 0.22 | 501 | 0.13 |
| 560 | 0.42 | 559 | 0.40 |
| 603 | 1.07 | 601 | 1.04 |
| 651 | 2.44 | 636 | 2.08 |
| 702 | 4.90 | 687 | 4.69 |
| 756 | 8.99 | 755 | 9.13 |

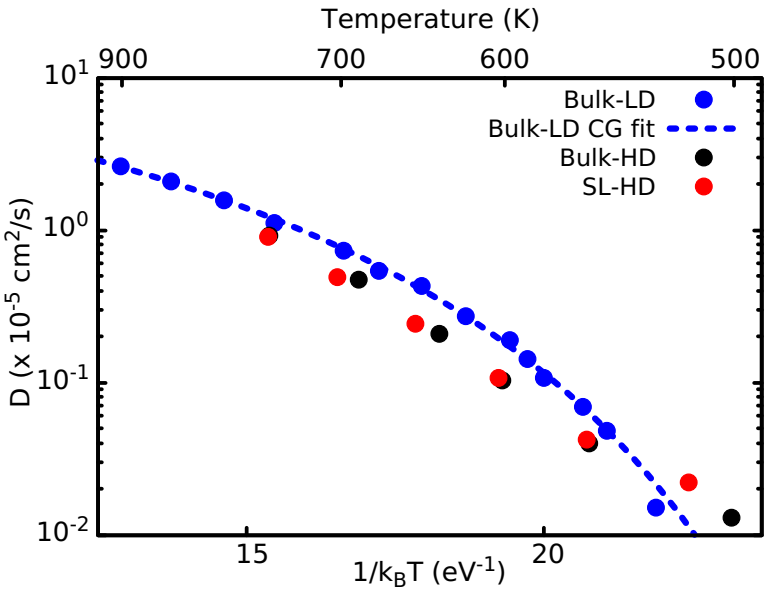


Figure S13: Diffusion coefficient $D$ ($10^{-5}$ cm$^2$/s) as a function of temperature from bulk NN+vdW simulations at the experimental density of the amorphous phase (bulk-LD) and of the crystalline hexagonal phase (bulk-HD) and of the superlattice model SL-HD (see article).

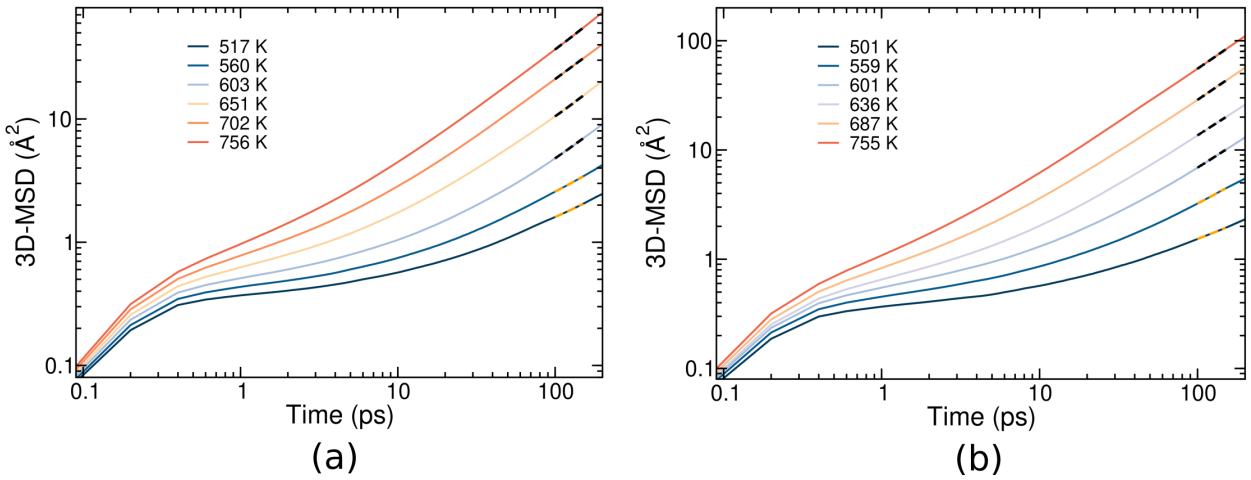


Figure S14: Mean square displacement (MSD) as a function of time from NVE simulations at the average temperatures given in the inset for (a) SL at the equilibrium density of the hexagonal phase (SL-HD) and (b) for the bulk at the same density (bulk-HD, see article). For the sake of comparison with the bulk, the 3D-MSD is plotted for the SL as well, where 3D-MSD= $3/2(< x^2 > + < y^2 >)$.

# References

(1) Abou El Kheir, O.; Bonati, L.; Parrinello, M.; Bernasconi, M. Unraveling the crystallization kinetics of the $Ge_2Sb_2Te_5$ phase change compound with a machine-learned interatomic potential. *npj Comput. Mater.* **2024**, *10*, 33.

(2) Stellhorn, J. R.; Hosokawa, S.; Kohara, S. Local- and Intermediate-Range Structures on Ordinary and Exotic Phase-Change Materials by Anomalous X-ray Scattering. *Anal. Sci.* **2020**, *36*, 5–9.

(3) Baker, D. A.; Paesler, M. A.; Lucovsky, G.; Agarwal, S. C.; Taylor, P. C. Application of Bond Constraint Theory to the Switchable Optical Memory Material $Ge_2Sb_2Te_5$. *Phys. Rev. Lett.* **2006**, *96*, 255501.

(4) Jóvári, P.; Kaban, L.; Steiner, J.; Beuneu, B.; Schöps, A.; Webb, A. 'Wrong bonds' in sputtered amorphous $Ge_2Sb_2Te_5$. *J Phys.: Condens. Matter* **2007**, *19*, 335212.

(5) Pethes, I.; Piarristeguy, A.; Pradel, A.; Michalik, J., S. Darpentigny; Zitolo, A.; Escalier, R.; Jóvári, P. Short-range order and topology of Te-rich amorphous Ge–Sb–Te alloys. *J. Amer. Ceramic Soc.* **2025**, *108*, e20258.

(6) Yong, Z.; Otani, A.; Maginn, E. J. Reliable Viscosity Calculation from Equilibrium Molecular Dynamics Simulations: A Time Decomposition Method. *J. Chem. Theory Comput.* **2015**, *11*, 3537–3546.

(7) Schumacher, M.; Weber, H.; Jóvári, P.; Tsuchiya, Y.; Youngs, T. G.; Kaban, I.; Mazzarello, R. Structural, electronic and kinetic properties of the phase-change material $Ge_2Sb_2Te_5$ in the liquid state. *Sci. Rep.* **2016**, *6*, 27434.